Out-of-equilibrium dynamics in round-trip and dissipation protocols

Francesco Tarantelli
francesco.tarantelli@phd.unipi.it

Tarantelli, Vicari PR B 105, 235124 (2022)
Tarantelli, Vicari PR B 108, 035128 (2023)
Franchi, Tarantelli PR B 108, 094114 (2023)
Tarantelli, Scopa PR B 108, 104316 (2023)

University of Pisa and INFN

17^{th} October

Introduction

- We address out-of-equilibrium dynamics of many-body systems subject to round-trip and dissipation protocols across quantum phase transitions;
- We perform quenched and Kibble-Zurek(KZ) protocols which develop dynamic scaling behavior at both the transitions obtained from a Renormalization Group(RG) framework;
- While classical and quantum models, belonging to the same universality class, show similar dynamic scaling frameworks, substantial differences emerge in the round-trip evolution;
- In the dissipation case, the Liouvillian gap plays a central role in the large-time regime.

Kitaev Model

Kitaev Hamiltonian mapped into a spin-$1/2$ XY chain, by a Jordan-Wigner transformation (OBC): $\hat{c} \longrightarrow \hat{\sigma}$

$$\hat{H}_K^{(\mathrm{ABC})} = -\sum_{x=1}^{L} \left[\left(\hat{c}_x^\dagger \, \hat{c}_{x+1} + \hat{c}_{x+1}^\dagger \, \hat{c}_x \right) + \delta \left(\hat{c}_x \, \hat{c}_{x+1} + \hat{c}_{x+1}^\dagger \, \hat{c}_x^\dagger \right) \right] - \sum_{x=1}^{L} \mu \, \hat{c}_x^\dagger \, \hat{c}_x \; ; \quad (1)$$

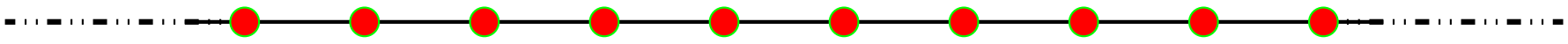

Continuous Transition point:

$$\mu_c = -2 \qquad \text{and} \qquad \delta = 1 \text{ fixed} \; ;$$

RG dimensions:

$$w = \mu - \mu_c \longrightarrow y_w = 1 \qquad \hat{c}_x \, , \; \hat{c}_x^\dagger \longrightarrow y_c = 1/2 \qquad \text{dynamic exp} : z = 1 \; .$$

Round - Trip

FT, E. Vicari PR B 105, 235124 (2022)
FT, S. Scopa PR B 108, 104316 (2023)

Kibble Zurek(KZ) Protocol

(i) Start at the equilibrium state (classical) and at the ground state $|\Psi(t = t_i)\rangle \equiv |\Psi(w_i < 0)\rangle$ (quantum);

(ii) quantum case:

$$\frac{d\,|\Psi(t)\rangle}{dt} = -i\hat{H}[w(t)]\,|\Psi(t)\rangle \;\; ;$$

(ii) classical one:

Metropolis algorithm;

$$\Downarrow$$

$$w(t) = t/t_s \;\; ;$$

from $w_i < 0$ to $w_f > 0$, where t_s is the time scale of the slow variations of w.

(iii) Then, for $t > t_f$, $w(t)$ decreases with the same t_s, from $w_f > 0$ to the original value $wi < 0$, closing the cycle.

Observables

Classical Ising model

$$M(t) = \frac{1}{L^2} \sum_i \langle S_i \rangle_t \;; \tag{2}$$

$$G(t, \boldsymbol{x}, \boldsymbol{y}) \equiv \langle s_{\boldsymbol{x}} \, s_{\boldsymbol{y}} \rangle_t \,. \tag{3}$$

Quantum models

Adiabaticity function:

$$A(t) = \Big| \langle \Psi_0[w(t)] | \Psi(t) \rangle \Big| \,; \tag{4}$$

Kitaev:

$$C(x,t) \equiv \langle \Psi(t) | \, c_j^\dagger c_{j+x} + c_{j+x}^\dagger c_j \, | \Psi(t) \rangle \;.$$

Dynamic scaling framework for the round-trip

The asymptotic dynamic FSS behavior is obtained by taking $t_s \to \infty$ and $L \to \infty$:

$$\begin{aligned} K &= w(t) L^{y_w}\,, & \Upsilon &= t_s / L^{\zeta}\,, \\ \Theta_i &= w_i\, t_s^{1-\kappa}\,, & \Theta &= w(t)\, t_s^{1-\kappa} = t / t_s^{\kappa}\,, \end{aligned} \tag{5}$$

where

$$\zeta = y_w + z\,, \qquad \kappa = z/\zeta\,, \qquad 1 - \kappa = y_w/\zeta\,. \tag{6}$$

with $w_f = -w_i = w_\star$, we have:

$$\Upsilon = t_s / L^{\zeta}\,, \quad \Theta = w(t)\, t_s^{1-\kappa}\,, \quad \Theta_\star = w_\star\, t_s^{1-\kappa}\,. \tag{7}$$

Numerical results - Classical Ising

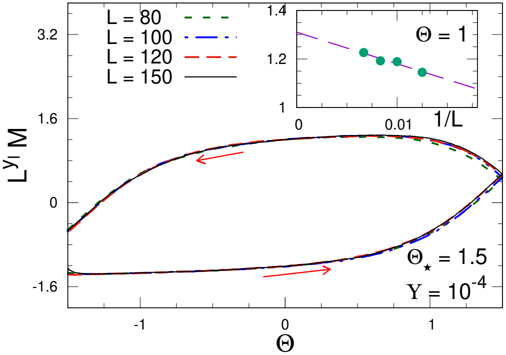

Figure 1:
$M^{(a/b)}(t, t_s, w_\star, L) \approx L^{-y_l}\mathcal{M}_i(\Upsilon, \Theta, \Theta_\star)$
$\Upsilon = 10^{-4}$, fixed $\Theta_\star = 1.5$ and plotted versus $\Theta = w(t)t_s^{1-\kappa}$.

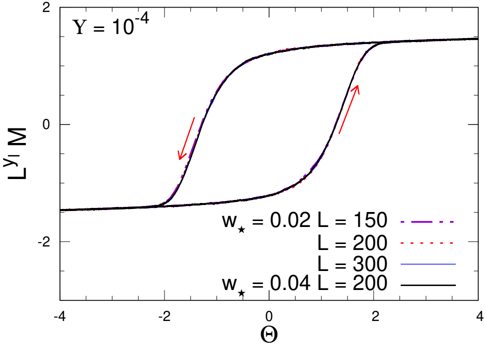

Figure 2: Thermalized classical state for fixed $\Upsilon = 10^{-4}$, and fixed $w_\star = 0.02$ and $w_\star = 0.04$.

Numerical results - Kitaev chain

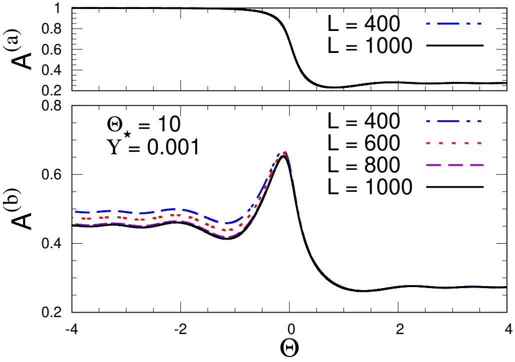

Figure 3: $A^{(a/b)}(t, t_s, w_\star, L) \approx \mathcal{A}^{(a/b)}(\Upsilon, \Theta, \Theta_\star)$; Finite $\Theta_\star = 10$ at fixed $\Upsilon = t_s/L^\zeta = 0.001$ and $\Theta_\star = w_\star L^{1-\kappa} = 10$, for outward and return.

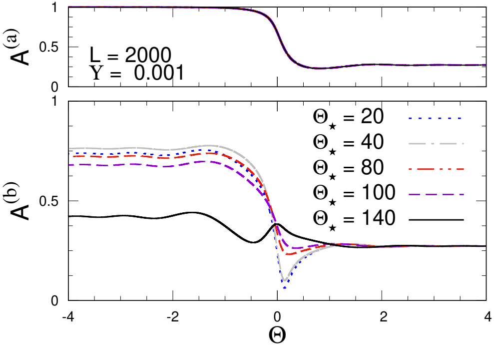

Figure 4: At $L = 2000$ and $\Upsilon = 0.001$ for the outward (top) and return (bottom), versus Θ, for various $\Theta_\star$.

The limit $\Theta_\star \to \infty$

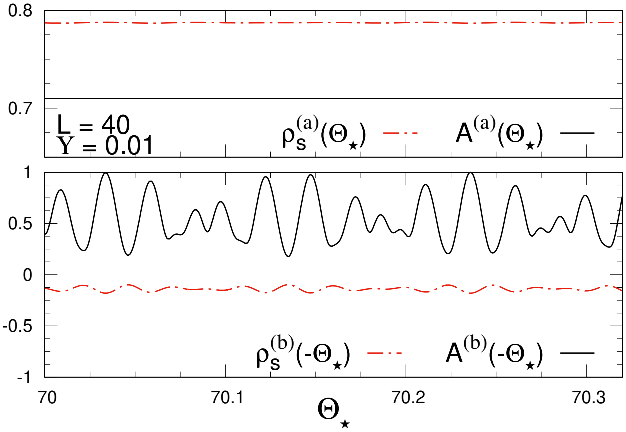

Figure 5: **Kitaev** - Fixed $L = 40$, $\Upsilon = 0.01$ versus $\Theta_\star$, close to $\Theta_\star = 70$. The top plot shows the values at $\Theta = \Theta_\star$, while the bottom at $\Theta = -\Theta_\star$.

Two-Level Model: $H_{2\ell}(t) = -\beta(t)\sigma^{(3)} + \frac{\Delta}{2}\sigma^{(1)}$

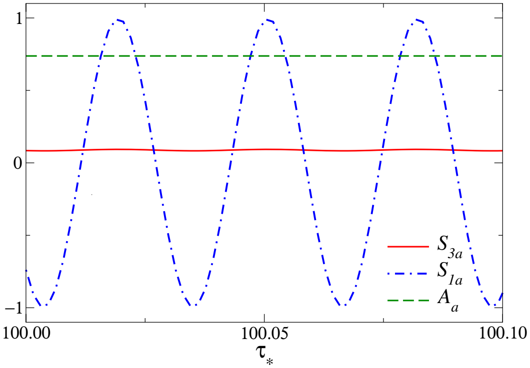

Figure 6: Dependence on $\tau_\star \equiv t_\star/\sqrt{t_s}$ at the end of the first dynamic branch for $\upsilon = 1$, and $\tau_\star \approx 100$.

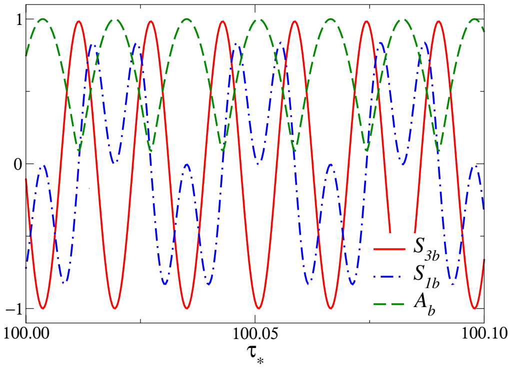

Figure 7: Dependence on $\tau_\star$ at the end of round-trip protocol for $\upsilon = t_s\Delta^2 = 1$, and $\tau_\star \approx 100$.

Dissipation

`A. Franchi, FT PR B 108, 094114 (2023)`

Lindblad framework

$$\frac{d\rho}{dt} = \mathcal{L}[\rho] = -i\Big[H, \rho\Big] + \mathbb{D}[\rho] \ ; \tag{8}$$

$\mathcal{L}$ is the Liouville superoperator, and $\mathbb{D}$ is the dissipation term with coupling w:

$$\mathbb{D}[\rho] = w \sum_{x \in \mathcal{I}} \mathbb{D}_x[\rho] \ , \tag{9}$$

$$\mathbb{D}_x[\rho] = \hat{L}_x \rho \hat{L}_x^\dagger - \frac{1}{2}\Big\{\rho, \hat{L}_x^\dagger \hat{L}_x\Big\} \ ; \tag{10}$$

Sunburst geometry

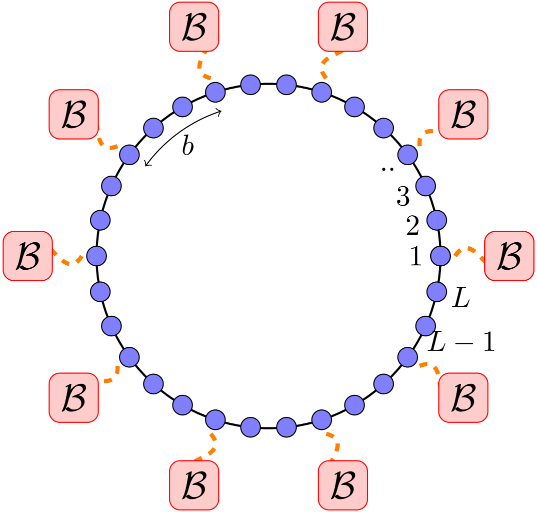

Liouvillian gap

$$\widetilde{\mathcal{L}}[\widetilde{\rho}_i] = \lambda_i \widetilde{\rho}_i \ , \qquad \lambda_i \in \mathbb{C} \ ; \tag{11}$$

$$\rho_{ij} \left|i\right\rangle \left\langle j\right| \longrightarrow \widetilde{\rho}_{ij} \left|i\right\rangle \left|j\right\rangle \ . \tag{12}$$

$$\widetilde{\mathcal{L}} = -i\big(\hat{H} \otimes \hat{\mathbb{I}} - \hat{\mathbb{I}} \otimes \hat{H}^t\big) + w \sum_{x \in \mathcal{I}} \hat{L}_x \otimes \hat{L}_x^* \tag{13}$$

$$- \frac{w}{2} \sum_{x \in \mathcal{I}} \big(\hat{L}_x^\dagger \hat{L}_x \otimes \hat{\mathbb{I}} + \hat{\mathbb{I}} \otimes \hat{L}_x^t \hat{L}_x^*\big) \ . \tag{14}$$

$$\Delta_\lambda = - \max_i \mathrm{Re}\lambda_i \ . \tag{15}$$

Interplay between local and homogeneous dissipation

The number of the external baths:

$$n \equiv L/b \; ; \tag{16}$$

b fixed $\longrightarrow$ local dissipation with $\Delta_\lambda \sim L^{-1} f(\mu, wL) \qquad L \to \infty$;

n fixed $\longrightarrow$ homogeneous dissipation with $\Delta_\lambda \sim L^{-3} \tilde{f}(\mu, w) \qquad L \to \infty$.

Liouvillian gap b fixed

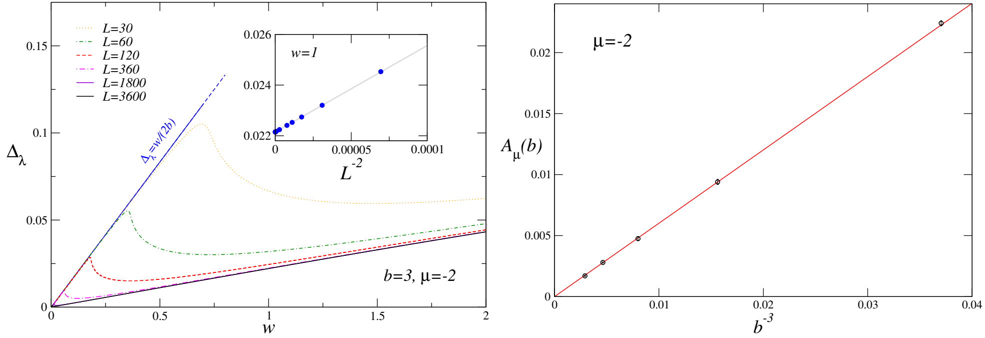

Figure 9: Liouvillian gap Δ_λ in terms of the dissipation coupling w for $b = 3$ and fixed $\mu = -2$.

$$\Delta_\lambda(w, b) = A_\mu(b)w\,, \quad A_\mu(b) = \frac{C_\mu}{b^3}\,, \quad w > w_*\,, \tag{17}$$

Liouvillian gap b fixed

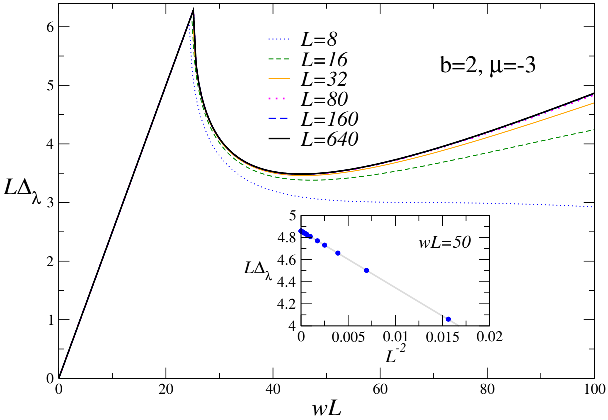

Liouvillian gap n fixed

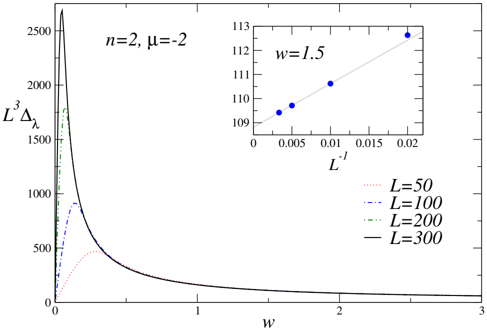

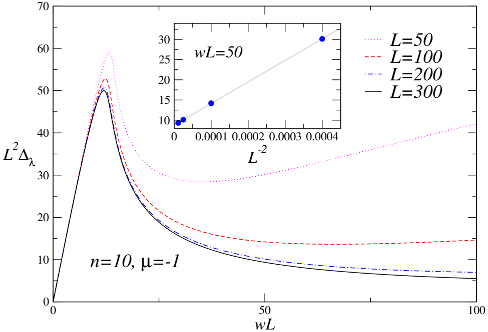

Dynamic Finite Size Scaling

The correlation function as observable:

$$C(x,y,t) \equiv \mathrm{Tr}[\rho(t)(\hat{c}_x^\dagger \hat{c}_y + \hat{c}_y^\dagger \hat{c}_x)]\,, \tag{18}$$

$$P(x,y,t) \equiv \mathrm{Tr}[\rho(t)(\hat{c}_x^\dagger \hat{c}_y^\dagger + \hat{c}_y \hat{c}_x)]\,. \tag{19}$$

The scaling parameters are set:

$$M_{i/f} = (\mu_{i/f} - \mu_c) L^{y_\mu} \qquad y_\mu = 1\ ; \tag{20}$$

$$\Theta = tL^{-z}\,,\ z = 1 \text{ for } t \sim L\ ; \qquad \Theta = t/\Delta_\lambda \text{ for } t \sim L^3\ ; \tag{21}$$

$$\gamma_b = \frac{wL^z}{b}\ . \tag{22}$$

The Scaling Laws can be expressed:

$$C(x,y,t) \approx L^{-2y_c} \mathcal{C}(M_i, M_f, \{X_i\}, \Theta, \gamma_b)\ ,$$

$$P(x,y,t) \approx L^{-2y_c} \mathcal{P}(M_i, M_f, \{X_i\}, \Theta, \gamma_b)\,.$$

Numerical Results

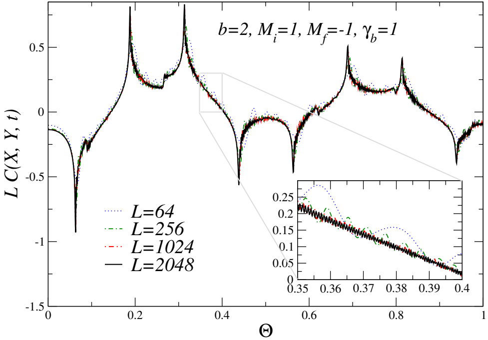

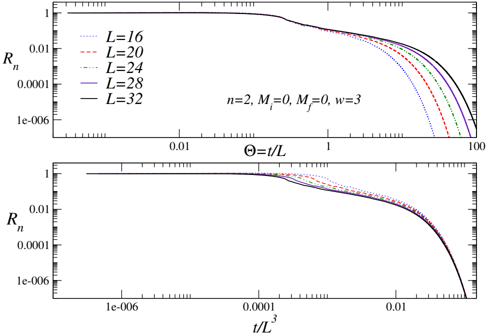

We introduce the RG invariant quantity R_n defined as

$$R_n = \frac{N(t) - N_{\text{asy}}}{N(0) - N_{\text{asy}}}\,, \tag{23}$$

where $N(t) = \sum_x^L \langle \hat{c}_x^\dagger \hat{c}_x(t) \rangle$ and $N_{\text{asy}} = \lim_{t\to\infty} N(t)$.

Conclusions

In the round-trip model:

- Analogy of the scaling behaviors at classical and quantum transitions is only partially extended to round-trip KZ protocols. Substantial differences emerge:
  1. classical systems develop scaling hysteresis-like scenarios,
  2. in quantum systems, the persistence of oscillating relative phases make the return way extremely sensitive to the parameters of the protocol;
- Even in the simple two-level quantum model, we have a similar behavior.

In the dissipation scenario:

- When we keep b fixed, the gap Δ_λ is always finite and depends linearly on the dissipation strength w ;
- Two different regimes:
  1. In the small w region, the gap is given by $\Delta_\lambda = w/(2b)$;
  2. At large w and sufficiently large b, $\Delta_\lambda = wC_\mu/b^3$ controls the gap in the large-size limit and the dynamic FSS.